



## Hydrogen production via water electrolysis on an active electrocatalyst: rGO/Ni nanocomposite

Didem BALUN KAYAN\*

Aksaray University, Faculty of Arts & Sciences, Department of Chemistry, Aksaray 68000, Türkiye

Received: 6 November 2022; Revised: 2 December 2022; Accepted: 5 December 2022

\*Corresponding author e-mail: [didembalun@gmail.com](mailto:didembalun@gmail.com)

**Citation:** Balun Kayan, D. *Int. J. Chem. Technol.* 2023, 7 (1), 1-5.

### ABSTRACT

The development of inexpensive and effective electrocatalyses are all-important for hydrogen production from water electrolysis. In this study, a facile design of a reduced graphene oxide (rGO) based electrocatalyst decorated with nickel nanoparticles is described. The voltammetric results and the hydrogen evolution reaction (HER) kinetics showed that the as-prepared nanocomposite is an effective and stable electrocatalyst for hydrogen production with a small Tafel slope of 152 mVdec<sup>-1</sup> and long-term continuous durability (over 24 h) in 0.5 M H<sub>2</sub>SO<sub>4</sub> solution. Also, the enhanced HER activity was confirmed by characterization results with the porous/greater electroactive surface area. The remarkable increase in electrocatalytic activity was due to the surface roughness and the synergistic chemical coupling effects between rGO and Ni nanoparticles.

**Keywords:** Hydrogen energy, water electrolysis, reduced graphene oxide, nickel nanoparticles.

### 1. INTRODUCTION

Energy demand and consequently environmental pollution increasing day by day. Hydrogen energy is viewed as a clean energy, alternative to the traditional fossil energy sources.<sup>1-6</sup> Although there are many production methods, water electrolysis is the most featured method because it is a cheap, sustainable and clean process.<sup>7-10</sup> So far, commercially available Pt/C is the most efficient electrocatalyst for the hydrogen evolution reaction (HER) but the use of these expensive catalysts does not allow viable operation of such processes on an industrial scale.<sup>11,12</sup> Inexpensive non-noble metal electrocatalysts are essential for successful

### Aktif bir elektrokatalizör üzerinde suyun elektroliziyle hidrojen üretimi: rGO/Ni nanokompozit

#### ÖZ

Suyun elektroliziyle hidrojen üretiminde ekonomik ve etkin elektrokatalizörlerin geliştirilmesi oldukça önemlidir. Bu çalışmada, nikel nanoparçacıklarla dekore edilmiş indirgenmiş grafen oksit (rGO) bazlı bir elektrokatalizörün basit bir tasarımı anlatılmaktadır. Voltametrik çalışmaların ve hidrojen oluşumu reaksiyonu (HER) kinetiğinin sonuçları, 152 mVdec<sup>-1</sup>’lık düşük Tafel eğimi ve 0,5 M H<sub>2</sub>SO<sub>4</sub> çözeltisi içinde uzun süreli gösterdiği dayanıklılıkla (24 saatin üzerinde), hazırlanan nanokompozitin hidrojen üretimi için etkili ve kararlı bir elektrokatalizör olduğunu göstermiştir. Ayrıca gözenekli/daha yüksek elektroaktif yüzey alanıyla HER aktivitesinin arttığını karakterizasyon sonuçları doğrulamıştır. Elektrokatalitik aktivitedeki dikkate değer artış, yüzey pürüzlülüğünden ve rGO ile Ni nanopartiküller arasındaki kimyasal etkileşmelerin sinerjik etkilerinden kaynaklanmaktadır.

**Anahtar kelimeler:** Hidrojen enerjisi, suyun elektrolizi, indirgenmiş grafen oksit, nikel nanopartikül.

hydrogen production.<sup>13-16</sup> As such, researchers have shifted their focus to base metals such as nickel (Ni), which are cheap yet exhibit high catalytic performance.<sup>17-20</sup> Trasatti plotted the logarithm of the exchange current density to the metal-hydrogen bond strength for various metals for hydrogen evolution reaction in acidic media. This diagram is known as a volcano diagram and allows us to compare the electrocatalytic activity of different metals on HER.<sup>21</sup> In this volcano plot, Ni is close to Pt, as an efficient catalyst for HER.<sup>22</sup> Besides, the use of metals in nanoscale not only provides to develop a cost-effective material, but also provides a more effective electrocatalyst with a high surface/volume ratio.<sup>23</sup> At

the same time, an appropriate support material plays a significant role for homogenous distribution of the metal catalyst and to demonstrate the effectiveness of it. As is known, the electrocatalytic activity of Ni can be increased with support materials or co-catalysts.<sup>24,25</sup> The reduced graphene oxide (rGO) is regarded as the catalyst support of choice due to its excellent properties of high specific surface area and superior electrical conductivity.<sup>26-29</sup> Furthermore, the effectual interaction between metal rGO increases the catalytic activity by increasing the active sites of the electrocatalyst.<sup>30</sup> Although there are many studies in the literature in which rGO is used as a supporting material for metal catalysts and numerous reduction methods for the preparation of rGO have been described,<sup>31-33</sup> developing a facile, low-cost and one-step method is still accepted as a challenge.

In this work, the surface of the glassy carbon electrode modified by reduced graphene oxide layer and then decorated with Ni nanoparticles, as an effective electrocatalyst for hydrogen evolution reaction in acidic media. As an alternative to the electrodes obtained by using many complex and expensive methods in the literature, the goal of this study is to obtain a new electrode surface for hydrogen evolution reaction by a simple, low cost and eco-friendly method. Linear sweep voltammetry (LSV) was used to get an idea about the electrocatalytic activity of rGO/Ni nanocomposite electrode for hydrogen evolution reaction. Then the Tafel polarization curves and electrochemical impedance spectroscopy (EIS) techniques were used to identify the electrode kinetics for HER. The morphology and elemental analysis of the electrode surface were carried out by scanning electron microscopy (SEM) and energy dispersive X-ray spectroscopy (EDS). Furthermore, the stability test of the rGO/Ni nanocomposite electrode was performed by chronopotentiometry technique.

## 2. MATERIALS AND METHODS

### 2.1. Materials

The chemicals and reagents of aqueous suspension of graphene oxide (GO), nickel sulphate ( $\text{Ni}_2\text{SO}_4$ ), sulfuric acid ( $\text{H}_2\text{SO}_4$ ), disodium hydrogen phosphate ( $\text{Na}_2\text{HPO}_4$ ) were purchased from Sigma-Aldrich and were used without further purification. Deionized water was used for all experiments.

### 2.2. Methods

The electrochemical measurements were performed by potentiostat (Gamry Interface 1000) in a classical three-electrode system in 0.5 M  $\text{H}_2\text{SO}_4$ . The electrochemical cell system consisted of a Pt wire (counter electrode), Ag/AgCl/ $\text{Cl}^-$  reference electrode and a modified GCE as an indicator electrode. The modified electrodes and the

bare electrode (for the comparison), tested for HER performance by LSV, EIS and Tafel polarization curves. The LSV tests were conducted in 0.5 M  $\text{H}_2\text{SO}_4$  at a sweep rate of  $10 \text{ mV s}^{-1}$ . The electrochemical impedance spectroscopy analysis was measured in the same electrochemical cell overpotential of -0.55V using frequency range between  $10^6$  and 0.1 Hz with 5 mV of AC amplitude voltage.

First the surface of the glassy carbon electrode (3 mm diameter) was mechanically polished with a solution of alumina powder ( $0.3 \mu\text{m}$ ). Then, the electrode was kept in ethanol for 5 minutes and then in an ultrasonic bath in distilled water for 5 minutes.  $7 \mu\text{L}$  of  $0.5 \text{ mg. mL}^{-1}$  graphene oxide solution was dropped onto the electrode surface and dried in an oven at  $70^\circ\text{C}$  for 15 minutes. The reduction of graphene oxide (rGO) was carried out by electrochemical reduction at a constant potential of -0.9 V [Ag/AgCl] for 900 s in 0.1 M phosphate buffer solution (pH=7). Also, the reduced graphene oxide surface decorated with nickel nanoparticles to achieve rGO/Ni surface.

In this case, the reduction of graphene oxide and nickel ions on the glassy carbon electrode surface was carried out simultaneously. After dropping  $7 \mu\text{L}$  of graphene oxide on the glassy carbon electrode it was dried as described above, then it was immersed in 0.1 M  $\text{Na}_2\text{HPO}_4$  solution (pH=4) containing 0.05 M  $\text{NiSO}_4$  and the reduction was performed at -0.9 V for 900s, so that the graphene oxide and  $\text{Ni}^{2+}$  ions were reduced simultaneously (rGO/Ni). All prepared electrodes were washed with distilled water and made ready for electrochemical measurements.

## 3. RESULTS AND DISCUSSION

### 3.1. Characterization Studies

The morphological properties of the electrode surfaces were analysed by SEM. Figure 1a shows the surface of the electrode coated with rGO, verifying the typical crumpled morphology. Figure 1b demonstrates the successful decoration of Ni nanoparticles onto rGO surface which is a major advantage for high electrocatalytic activity. Figure 1b, 1c and 1d are the different magnification images of rGO/Ni surface, which reveal the uniform distribution of Ni nanoparticles with multiple pores. The high magnification image shows distinctly the rough surface of the electrocatalyst. The size of the particles are in the range of 100-200 nm. It is well known that this bumpy surface provides more active sites which increases the accessibility of the  $\text{H}^+$  ions, consequently the electrochemical performance of the catalyst.<sup>34</sup> Such a surface also facilitates the evolution of hydrogen gas bubbles. The chemical composition of the rGO/Ni composite film was evaluated by EDS and obtained spectrum is shown in Figure 2. The presence of carbon,

oxygen and nickel peaks with mass and atomic percentage ratios are indicated in the EDS spectrum.

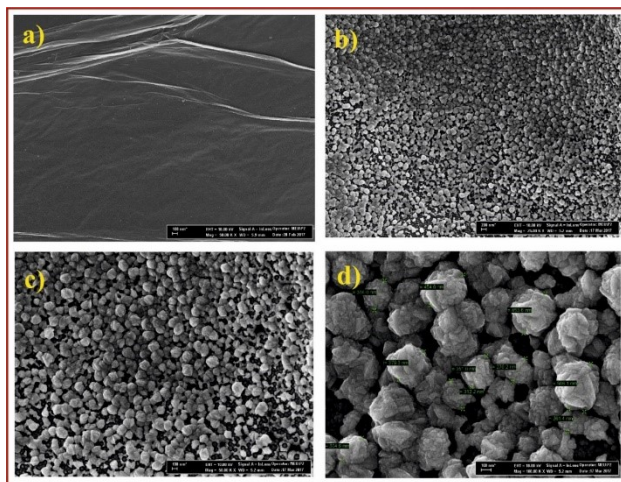


**Figure 1.** SEM images of rGO (a) and rGO/Ni surface with different magnifications (b-d).

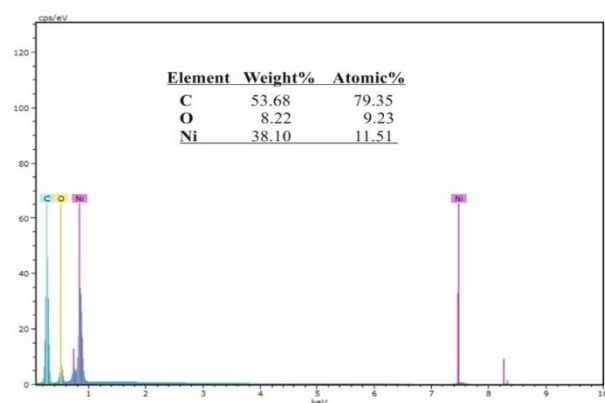


**Figure 2.** The EDS spectrum of rGO/Ni composite film.

### 3.2. Electrochemical Studies

The HER performances of the rGO and rGO/Ni nanoparticles coated electrodes first investigated with linear sweep voltammetry (Figure 3) in the potential range of -0.2 V and -0.8V. The polarization curve for GCE also obtained, for comparison. Data from LSV have demonstrated that the electron transfer rate in the Ni decorated composite film is fast, compatible with the high catalytic activity of the Ni particles. The catalytic performance of the rGO/Ni electrode was based upon to the structuration of the composite, which caused a homogenous distribution of the Ni nanoparticles on the rGO, as shown by SEM micrograph. Well dispersion of Ni nanoparticles on the rGO surface provides a large active surface area for  $H^+$  adsorption, and it leads the higher current density, as expected.

After LSV studies, Tafel polarization curves (current-potential diagrams) of the electrodes were evaluated and the results given in the Figure 4.

From the Tafel polarization curves, it is seen that the highest current density is obtained on the GCE/rGO/Ni electrode. The calculated Tafel slopes were 249, 178 and 152  $mV\ dec^{-1}$ , respectively. The Tafel slope denoted by  $b$ , derived from Tafel equation ( $\eta = a + b \log i$ ), provides important information about electrode kinetics and expresses as  $mV$  per decade ( $mV.decade^{-1}$ ) of current.<sup>35</sup> The smaller slope, requires lower overpotential to get higher current densities. It seems clearly that, the calculated Tafel slopes are reduced when the electrode surface modified with rGO and then Ni nanoparticles. The decrease in Tafel slopes is an evidence of the enhancing the electrocatalytic activity for HER.<sup>36,37</sup>

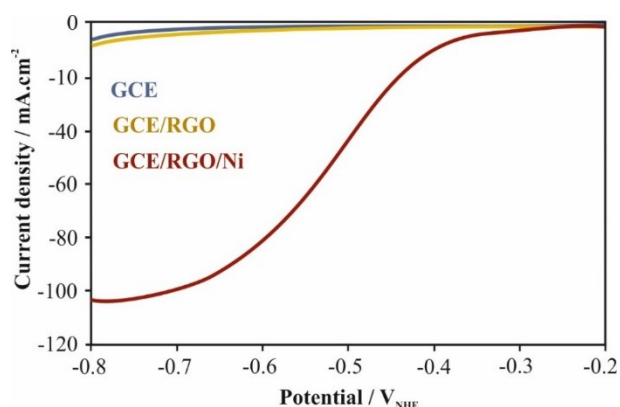


**Figure 3.** LSV of bare GCE, GCE/rGO and GCE/rGO/Ni electrodes recorded in 0.5 M  $H_2SO_4$  solution ( $v = 10\ mV\ s^{-1}$ ).

Another important parameter obtained for HER kinetics from Tafel plots is the required overpotential ( $\eta_{10}$ ) to achieve  $10\ mA.cm^{-2}$  current density.<sup>6,38</sup> A smaller  $\eta_{10}$  indicates a higher catalytic performance. It can be seen from Figure 4 that the GCE/rGO/Ni exhibited the best HER activity with the smallest overpotential (0.475 V) required at  $10\ mA.cm^{-2}$ .

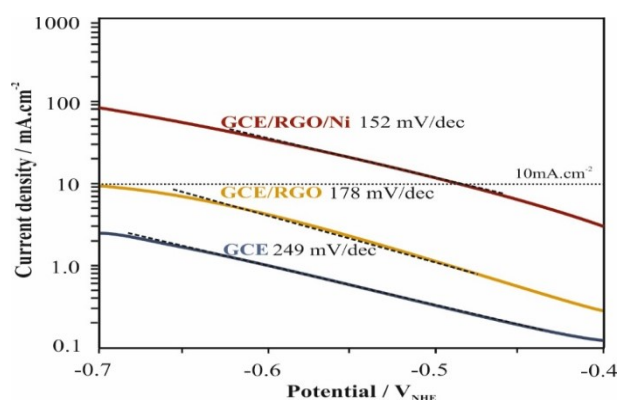


**Figure 4.** Current-potential diagrams (Tafel curves) of bare GCE, GCE/rGO and GCE/rGO/Ni electrodes recorded in 0.5 M  $H_2SO_4$  electrolyte medium ( $v: 1\ mVs^{-1}$ ).

The HER performances of the electrode surfaces also examined by electrochemical impedance spectroscopy measurements. The EIS results are shown as Nyquist diagrams in Figure 5 to better understand the electrochemical behaviour of rGO and rGO/Ni coated

electrodes. The semi-circle obtained from Nyquist plots have been simulated with the Randles equivalent circuit which shown as inset in Figure 5, consisted of electrolyte resistance ( $R_e$ ), a constant phase element (CPE) used instead of a double layer capacitance ( $C_{dl}$ ), in order to give a more accurate fit to the experimental results. The calculated double layer capacitance values were 9.03 and 1.22  $\text{mF}\cdot\text{cm}^{-2}$  for rGO/Ni coated and rGO coated electrodes respectively. This result confirms the higher hydrogen adsorption of the porous structure which leads the higher electrocatalytic performance for hydrogen evolution.

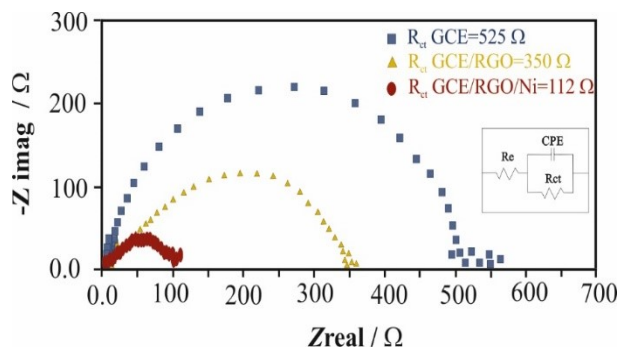


**Figure 5.** Nyquist diagrams of bare GCE, GCE/rGO and GCE/rGO/Ni electrodes recorded in 0.5 M  $\text{H}_2\text{SO}_4$  at -0.55V.

The real and the imaginary impedance of the rGO/Ni coated electrode are significantly lower than that of the rGO coated electrode. The charge transfer resistance for hydrogen formation was calculated for bare GCE as 525 $\Omega$ , it decreases to 350  $\Omega$  on the rGO coated electrode and to 112  $\Omega$  on the rGO/Ni coated electrode. The values of  $R_{ct}$  can be represented for the total reaction resistance, and lower reaction resistance means higher electrocatalytic performance for HER.<sup>39-40</sup>

### 3.3. Stability Studies

We also investigated the HER performance of the as-prepared electrode by stability tests. The long-term stability of rGO/Ni nanocomposite was tested at -0.7 V, the result shown in Figure 6 revealed that the as-prepared electrode can work continuously for  $\geq 24$  h with a slight decrease.

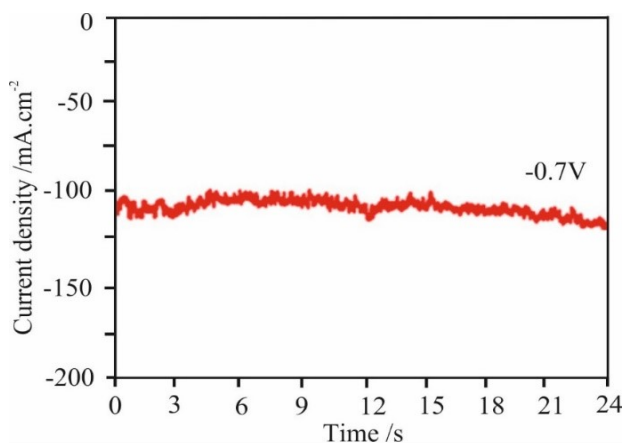


**Figure 6.** Long-term stability test of rGO/Ni coated electrode in 0.5 M  $\text{H}_2\text{SO}_4$  at -0.7V.

## CONCLUSIONS

An efficient electrocatalyst, based on reduced graphene oxide (rGO) decorated with Ni nanoparticles was synthesized by a facile method in this study. The synthesized nanocomposite was characterized by SEM and EDS techniques. The Ni nanoparticles were found to be uniformly distributed on the rGO sheets which had high surface area. The electrocatalytic activity of the nanocomposite investigated for hydrogen production, by electrochemical measurements; by LSV, Tafel extrapolation curves and EIS. High electrocatalytic activity was observed for the rGO/Ni nanocomposite, with a Tafel plot slope of 152  $\text{mV dec}^{-1}$ , a low charge transfer resistance of 112  $\Omega$  and a long-term stability over 24 h at -0.7V. These results demonstrate that this nanocomposite which synthesized by a facile and cost-effective way, is a promising catalyst for applications water electrolysis to produce hydrogen.

## ACKNOWLEDGEMENTS

The author is grateful to Aksaray University Scientific Research Projects Coordination Unit (ASU-BAP, 2016-034) for financial support.

## Conflict of interest

*I declare that there is no a conflict of interest with any person, institute, company, etc.*

## REFERENCES

- Razi, F.; Dincer, I. *Renew. Sustain. Energy Rev.* **2022**, 168, 112763- 112775.
- Qureshi, F.; Yusuf, M.; Kamyab H.; Zaidi, S. Khalil M. J.; Khan, M. A.; Alam, M.A.; Masood F.; Bazli, L.; Chelliapan.; Abdullah, B. *Sustain. Energy Technol. Assess.* **2022**, 53, 102677-102694.
- Wang, S.; Wu, X.; Jafarmadar S.; Singh, P.K.; Khorasani, S.; Marefati, M.; Alizadeh, A. *J. Energy Storage* **2022**, 54, 105274- 105290.
- Zahedi, R.; Ghodusinejad, M. H.; Aslani, A.; Hachem-Vermette, C. *Energy Strategy Rev.* **2022**, 43, 100930-100946.
- Ang, T-Z.; Salem, M.; Kamarol, M.; Das, H.S.; Nazari, M.A.; Prabakaran, N. *Energy Strategy Rev.* **2022**, 100939-100964.
- Balun Kayan, D.; Baran, T.; Menteş, A. *Electrochim. Acta*, **2022**, 422, 140513-140520.

7. Yu, Z.-Y.; Duan, Y.; Feng, X.-Y.; Yu, X.; Gao, M.-R.; Yu, S.-H. *Adv. Mater.* **2021**, *33*, 2007100-20071034.
8. Ahmed, S. F.; Mofijur, M.; Nuzhat, S.; Rafa, N.; Musharrat, A.; Lam, S.S.; Boretti, A. *Int. J. Hydrog. Energy*, **2022**, *47*(88), 37227-37255
9. Vidas, Leonardo; Castro, Rui. *Applied Sciences*, **2021**, *11*(23), 11363-11389.
10. Kamaroddin, M.F.A.; Sabli, N.; Abdullah T.A.T.; Siajam, S.I.; Abdullah, L.C.; Jalil A.A.; Ahmad, A. *Membranes*, **2021**, *11*(810), 1-28.
11. Yao, R.-Q.; Zhou, Y.-T.; Shi, H.; Wan, W.-B.; Zhang, Q.-H.; Gu, L.; Zhu, Y.-F.; Wen, Z.; Lang, X.-Y.; Jiang, Q. *Adv. Func. Mat.* **2021**, *31*(10), 2009613-2009621.
12. Liu, C.; Song, H.; Dai, Z.; Xiong, Y. *Ionics*, **2022**, *28*(3), 1311-1321.
13. Cao, Z.; Song, H.; Liu, C.; Tang, W.; Liu J.; Yang, B.; Xie, W.; Yu, Z. *Electrocatalysis*, **2022**, *13*, 807-817.
14. Kumar, S.S.; Lim, H. *Energy Reports*, **2022**, *8*, 13793-13813.
15. Theerthagiri, J.; Lee, S. J.; Murthy, A.P.; Madhavan, J.; Choi, M.Y. *Curr. Opin. Solid State Mater. Sci.* **2020**, *24*(1), 100805-100826.
16. Wu, T.; Sun, M.Z.; Huang, B.L. *Rare Metals*, **2022**, *41*, 2169-2183
17. Ji, L.; Lv, C.; Chen, Z.; Huang, Z.; Zhang, C. *Adv. Mater.* **2018**, *30*(17), 1705653-1705659.
18. Chen, Z.; Wei, W.; Ni, B.J. *Curr. Opin. Green Sustain. Chem.* **2021**, *27*, 100398-100405.
19. Wu, H.; Feng, C.; Zhang, L.; Zhang, J.; Wilkinson, D.P. *Electrochem. Energy Reviews* **2021**, *4*(3), 473-507.
20. Guo, M.; Song, S.; Zhang, S.; Yan, Y.; Zhan, K.; Yang, J.; Zhao, B. *ACS Sustain. Chem. Eng.* **2020**, *8*(19), 7436-7444.
21. Trasatti, S. *J. Electroanal. Chem.* **1972**, *39*, 163-184.
22. Jin, H.; Liu, X.; Chen, S.; Vasileff, A.; Li, L.; Jiao, Y.; Song, L.; Zheng, Y.; Qiao, S.-Z.; ACS Energy Lett. **2019**, *4*, 4, 805-810
23. Chang, H.; Shi, L.N.; Chen, Y.H.; Wang, P.F.; Yi, T.F. *Coord. Chem. Rev.* **2022**, *473*, 214839-214870.
24. Zaher, A.; El Rouby, W.M.; Barakat, N.A. *Fuel*, **2020**, *280*, 118654.
25. Liu, G.; Hou, F.; Peng, S.; Wang, X.; Fang, B. *Nanomaterials* **2022**, *12*(17), 2935-2947.
26. Askari, M.B.; Rozati, S.M.; Salarizadeh, P.; Azizi, S. *Ceramics International*, **2022** *48*(11), 16123-16130.
27. Karimi, A.; Kazeminezhad, I.; Naderi, L.; Shahrokhian, S. *J. Phys. Chem. C.*, **2020**, *124*(8), 4393-4407.
28. Wan, Z., Bai, X., Mo, H., Yang, J., Wang, Z., Zhou, L. *Colloids Surf A Physicochem Eng Asp.* **2021**, *614*, 126048-126059.
29. Zhao, X.; Luo, D.; Wang, Y.; Liu, Z.H. *Nano Res.* **2019**, *12*(11), 2872-2880.
30. Xu, Q.; Zang L.; Li, Z.; Shen, F.; Zhang, Y.; Sun, L.; *Int. J. Hydrog. Energy*, **2022**, *47*(91), 38571-38582.
31. Wu, J.; Wang, J.; Huang, X.; Bai, H. *Energy Environ. Sci.* **2018**, *11*(5), 1280-1286.
32. Rafiee, M.; Nitzsche, F.; Laliberte, J.; Hind, S.; Robitaille, F.; Labrosse, M.R. *Compos. B: Eng.* **2019**, *164*, 1-9.
33. Qian, H.; Wang, J.; Yan, L. *J. Bioresour. Bioprod.* **2020**, *5*(3), 204-210.
34. Nairan, A.; Liang, C.; Chiang, S.W.; Wu, Y.; Zou, P.; Khan, U.; Liu, W.; Kang F.; Guo S.; Wu, J.; Yang, C. *Energy Environ. Sci.* **2021**, *14*(3), 1594-1601.
35. Murthy, A.P.; Theerthagiri, J.; Madhavan, J. *J. Phys. Chem. C.* **2018**, *122*(42), 23943-23949.
36. Wu, L.; Hoof, A. J. F.; Dzade N.Y.; Gao L.; Richard M.-I.; Friedrich H.; Leeuw N.H.D.; Hensen E.J.M.; Hofmann J. P. *Phys. Chem. Chem. Phys.* **2019**, *21*, 6071-6079.
37. Najafi, L.; Bellani, S.; Oropesa-Nuñez, R.; Ansaldo, A.; Prato M.; Castillo, A. E. D.R.; Bonaccorso F. *Adv. Energy Mater.* **2018**, *8*, 1703212-1703227.
38. Zeng M.; Li, Y. *J. Mater. Chem. A*, **2015**, *3*, 14942-14962
39. Balun Kayan, D.; İlhan, M.; Koçak, D. *Ionics*, **2018**, *24*(2), 563-569.
40. Wang, X.; Zhou, H.; Zhang, D.; Pi, M.; Feng, J.; Chen, S. *J. Power Sources.* **2018**, *387*, 1-8.